

# Geophysical Research Letters®



## RESEARCH LETTER

10.1029/2023GL108096

## Linking Upwelling Dynamics and Subsurface Nutrients to Projected Productivity Changes in the California Current System

### Key Points:

- Future changes in the California Current System are evaluated using an ensemble of downscaled ocean projections
- We evaluate changes in Ekman and geostrophic transports, water column structure, and subsurface nitrate concentrations
- Across models, phytoplankton biomass changes are more closely tied to subsurface nitrate concentration than upwelling strength

Michael G. Jacox<sup>1,2</sup> , Steven J. Bograd<sup>1</sup> , Jerome Fiechter<sup>3</sup>, Mercedes Pozo Buil<sup>1,4</sup>, Michael Alexander<sup>2</sup> , Dillon Amaya<sup>2</sup> , Nathali Cordero Quiros<sup>1,4</sup> , Hui Ding<sup>2,5</sup> , and Ryan R. Rykaczewski<sup>6</sup> 

<sup>1</sup>Ecosystem Science Division, Southwest Fisheries Science Center, National Oceanic and Atmospheric Administration, Monterey, CA, USA, <sup>2</sup>Physical Science Laboratory, Earth System Research Laboratories, National Oceanic and Atmospheric Administration, Boulder, CO, USA, <sup>3</sup>Ocean Sciences Department, University of California Santa Cruz, Santa Cruz, CA, USA, <sup>4</sup>Institute of Marine Sciences, University of California Santa Cruz, Santa Cruz, CA, USA, <sup>5</sup>University of Colorado Boulder, Boulder, CO, USA, <sup>6</sup>Ecosystem Sciences Division, Pacific Islands Fisheries Science Center, National Oceanic and Atmospheric Administration, Honolulu, HI, USA

### Supporting Information:

Supporting Information may be found in the online version of this article.

### Correspondence to:

M. G. Jacox,  
michael.jacox@noaa.gov

### Citation:

Jacox, M. G., Bograd, S. J., Fiechter, J., Pozo Buil, M., Alexander, M., Amaya, D., et al. (2024). Linking upwelling dynamics and subsurface nutrients to projected productivity changes in the California Current System. *Geophysical Research Letters*, 51, e2023GL108096. <https://doi.org/10.1029/2023GL108096>

Received 28 DEC 2023

Accepted 27 MAR 2024

**Abstract** Given the importance of coastal upwelling systems to ocean productivity, fisheries, and biogeochemical cycles, their response to climate change is of great interest. However, there is no consensus on future productivity changes in these systems, which may be controlled by multiple drivers including wind-driven and geostrophic transport, stratification, and source water properties. Here we use an ensemble of regional ocean projections and recently developed upwelling indices for the California Current System to disentangle these sometimes-competing influences. Some changes are consistent among models (e.g., decreased mixed layer depth), while for others there is a lack of agreement even on the direction of future change (e.g., nitrate concentration in upwelled waters). Despite models' diverging projections of productivity changes, they agree that those changes are predominantly driven by subsurface nitrate concentrations, not by upwelling strength. Our results highlight the need for more attention to processes governing subsurface nutrient changes, not just upwelling strength.

**Plain Language Summary** The California Current System is one of the world's eastern boundary upwelling systems—some of the most productive regions in the global ocean. These regions support a wide range of human activities, such as fisheries and tourism, motivating extensive research on how they might evolve under future climate change. A number of hypotheses have been offered to describe future physical and chemical change in these systems, and in terms of their impacts on primary production (which forms the base of the marine food web), these mechanisms may reinforce or oppose each other. Enhanced nutrient concentrations in upwelling source waters would support higher productivity, increased stratification would limit nutrient supply and productivity, and increased upwelling could enhance productivity to a point but limit productivity if it is too strong. There is no consensus on which mechanism(s) will predominantly drive future productivity changes. Here we provide a detailed analysis of projected physical and biogeochemical changes and how they relate to productivity changes. Even though different models project different futures, we find that in all of them the primary control on productivity is the nitrate concentration of subsurface waters, not the strength of upwelling, which has received more attention to date.

## 1. Introduction

As some of the most biologically productive regions in the global ocean, eastern boundary upwelling systems (EBUS) hold significant ecological, economic, and cultural value. It is no surprise, then, that extensive effort has been applied toward understanding how these regions will be affected by anthropogenic climate change. Future changes in EBUS have the potential to impact, for example, the carbon cycle, populations and distributions of marine species, and commercial and recreational fisheries (e.g., Bograd et al., 2023; Doney et al., 2012; Garcia-Reyes et al., 2015 and references therein).

Despite intense interest in their future evolution, projected changes in the productivity of EBUS are decidedly uncertain (Bograd et al., 2023). This uncertainty can be traced to the array of potential physical and

© 2024 The Authors. This article has been contributed to by U.S. Government employees and their work is in the public domain in the USA.

This is an open access article under the terms of the [Creative Commons Attribution-NonCommercial-NoDerivs License](https://creativecommons.org/licenses/by/4.0/), which permits use and distribution in any medium, provided the original work is properly cited, the use is non-commercial and no modifications or adaptations are made.

biogeochemical conditions that modulate primary production in EBUS. In brief, potential mechanisms governing future productivity include changes to (a) the strength of wind-driven Ekman transport due to shifting intensities and locations of atmospheric pressure systems (Bakun, 1990; Rykaczewski et al., 2015; Schmidt et al., 2020; Wang et al., 2015), (b) cross-shore geostrophic transport, which can also modulate upwelling intensity (Cheresh & Fiechter, 2020; Ding et al., 2021; Jing et al., 2023; Oerder et al., 2015), (c) upper-ocean stratification (Cordero-Quiros et al., 2022) and associated shoaling of the mixed layer (Amaya et al., 2021; Shi et al., 2022) altering the source depth and efficacy of upwelling, and (d) source water chemistry, in particular nitrate concentration, owing to alterations in basin-scale ocean circulation and ventilation (Cheresh et al., 2023; Howard et al., 2020; Pozo Buil et al., 2021; Rykaczewski & Dunne, 2010). In terms of their effects on primary productivity, these various processes may act in concert or in opposition; discrepancies in their evolution underlie the lack of climate model agreement on future change in EBUS productivity (Bograd et al., 2023; Garcia-Reyes et al., 2015).

The purpose of this study is to provide a comprehensive analysis of physical and biogeochemical changes modulating projected productivity in the California Current System (CCS), one of the world's major EBUS. We leverage recently developed upwelling indices for the U.S. west coast (Jacox et al., 2018) and high-resolution regional ocean projections (Pozo Buil et al., 2021), which can improve the representation of EBUS under climate change (Chang et al., 2023; Jing et al., 2023). Our aim is not to definitively state how the CCS will change, but to identify the key process(es) that underlie future change and, thus, must be understood to better constrain future change.

## 2. Methods

### 2.1. Regional Ocean Projections

Projected future changes in ocean conditions were derived from an ensemble of regional projections for the CCS, described in detail in Pozo Buil et al. (2021). The regional model is the Regional Ocean Modeling System (ROMS) coupled to a biogeochemical model based on the North Pacific Ecosystem Model for Understanding Regional Oceanography (NEMURO; Kishi et al., 2007), with both ROMS and NEMURO specifically tailored to the CCS by the UC Santa Cruz (UCSC) ocean modeling group (Cheresh & Fiechter, 2020; Fiechter et al., 2018; Veneziani et al., 2009). We refer to the CCS ocean-biogeochemical model as ROMS-NEMUCSC. The domain spans 134–115.5°W and 30–48°N, with a horizontal resolution of 0.1° and 42 terrain-following vertical levels (Figure 1a). Earth System Model (ESM) forcing was obtained from three models contributing to the CMIP5 ensemble under the high-emission RCP8.5 scenario. The models are from the Geophysical Fluid Dynamics Laboratory (GFDL-ESM2M; hereafter GFDL), Institut Pierre-Simon Laplace (IPSL-CM5A-MR; hereafter IPSL), and Hadley Center (HadGEM2-ES; hereafter HAD). ESM output was bias-corrected using a time-varying delta method in which the monthly change from the ESM is added to a high-resolution historical climatology (Drenkard et al., 2021; Pozo Buil et al., 2021). The historical climatologies were derived from the Simple Ocean Data Assimilation v2.1.6 (Carton & Giese, 2008) for ocean physics, from the European Center for Medium-Range Weather Forecasts version 5 (ERA-5; Hersbach et al., 2020) and Cross-Calibrated Multi-Platform winds (CCMP1; Atlas et al., 2011) for surface forcing, and from the World Ocean Atlas climatology (Garcia et al., 2010a, 2010b) for nutrients and oxygen. Model runs span the period 1980–2100 and we start our analysis in 1991, avoiding any potential spin-up effects in the regional model.

### 2.2. Upwelling-Relevant Physical and Biogeochemical Variables

Historical conditions and future changes relevant to upwelling were characterized using a suite of physical and biogeochemical conditions (Figure 1b) obtained from the regional ocean projections. These variables, detailed below, were chosen to characterize not just upwelling itself but also its individual components, as well as water column and nutrient characteristics that control the efficacy of upwelling (i.e., the nutrient supplied to the surface mixed layer by upwelling).

Upwelling transport is characterized using the Coastal Upwelling Transport Index (CUTI), which is a measure of the vertical volume transport through the base of the mixed layer in a coastal band along the U.S. west coast. CUTI is defined as the sum of two components—Ekman transport and geostrophic transport—both of which influence upwelling strength (Figure 1b). The theory and methodology behind CUTI are described in detail in Jacox et al. (2018); we provide a brief summary here.

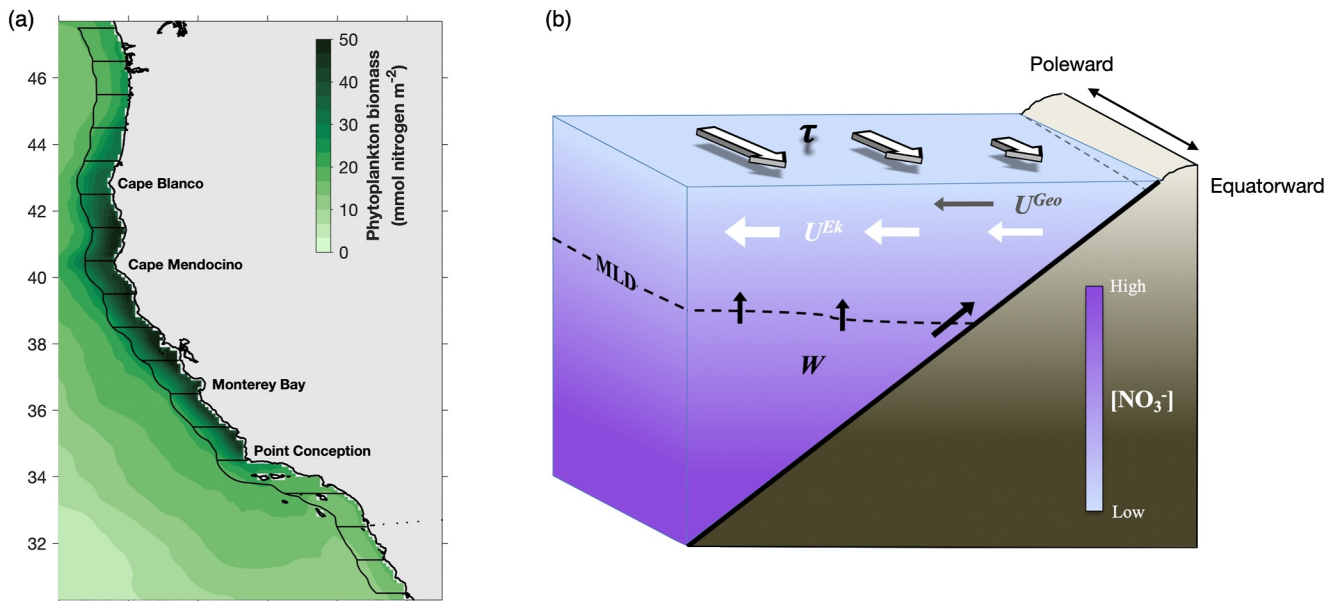


**Figure 1.** (a) Study domain showing the ensemble mean historical phytoplankton biomass from the downscaled simulations, integrated over the upper 50 m and averaged March–August 1991–2020. Black contours outline one-degree latitude bins extending 75 km offshore used to calculate upwelling and associated conditions. (b) Schematic showing upwelling-relevant parameters including surface wind stress ( $\tau$ ), Ekman transport ( $U^{Ek}$ ), geostrophic transport ( $U^{Geo}$ ), vertical transport ( $W$ ), mixed layer depth (MLD), and nitrate concentration ( $[NO_3^-]$ ). All transports are defined such that positive is upwelling favorable (i.e., offshore is positive for  $U^{Ek}$  and  $U^{Geo}$ , upward is positive for  $W$ ). Panel (b) modified from Bograd et al. (2023).

Ekman transport is a combination of (a) coastal divergence, in which equatorward (poleward) surface winds move water in the surface mixed layer away from (toward) the coast, leading to upwelling (downwelling) at the coastal boundary and (b) Ekman pumping/suction, in which positive (negative) wind stress curl induces divergence (convergence) in the surface mixed layer and consequently upwelling (downwelling) that can occur away from the coastal boundary. We calculate the total wind-driven upwelling by integrating Ekman transport around the perimeter of one-degree latitude bands, each extending 75 km offshore to cover the coastal band of elevated primary production (Figure 1a; Jacox et al., 2016). By integrating the Ekman transport around each region, we implicitly capture both coastal divergence and curl-driven upwelling without attempting to separate the two.

Cross-shore geostrophic flow, associated with an alongshore pressure gradient, can either enhance or counter the Ekman transport component of upwelling (Colas et al., 2008; Marchesiello & Estrade, 2010). In general, the geostrophic component along the U.S. west coast tends to be of opposite sign and smaller magnitude compared to the Ekman component (Jacox et al., 2018). Geostrophic transport is calculated from the sea surface height gradient and mixed layer depth (MLD), with the latter defined by a density change corresponding to a 0.8°C change in temperature (Jacox et al., 2018; Kara et al., 2000). As for Ekman transport, we integrate geostrophic transport around the perimeter of each one-degree box to obtain its total contribution to upwelling.

Our analysis of upwelling-related biogeochemical changes focuses on concentrations of nitrate—the major limiting macronutrient in the CCS (Deutsch et al., 2021; Messié & Chavez, 2015)—and of small (nanophytoplankton), large (diatom), and total phytoplankton biomass, a proxy for primary production. Each of these variables is explicitly represented in ROMS-NEMUCSC and can be obtained directly from the model. Nitrate flux into the surface mixed layer (represented by the Biologically Effective Upwelling Transport Index (BEUTI), or BEUTI; Jacox et al., 2018) is calculated as the product of vertical transport (CUTI) and nitrate concentration at the base of the mixed layer. Phytoplankton biomasses are integrated over the upper 50 m of the water column, though our results are not sensitive to this choice of integration depth. Much of our analysis focuses on the core CCS upwelling season (March–August; Jacox et al., 2016), though results throughout the annual cycle are discussed (Section 3.3).

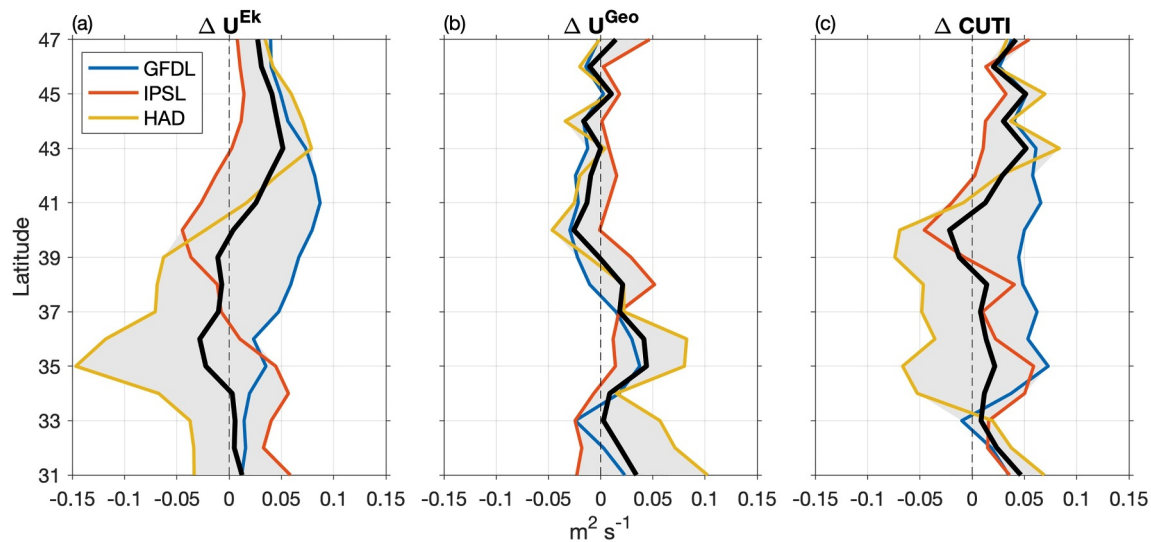


**Figure 2.** Projected upwelling season (March–August) changes in (a) Ekman, (b) geostrophic, and (c) total vertical transport (Coastal Upwelling Transport Index) between historical (1991–2020) and future (2071–2100) epochs. Transport metrics are calculated for bins spanning 1 degree of latitude and extending 75 km offshore (Figure 1a). For all transport changes, positive values are upwelling favorable. Colored lines show projections forced by different ESMs, with the ensemble mean shown in black and ensemble spread in gray shading.

### 2.3. Calculating Change

Future changes are shown as differences between 30-year epochs representing recent historical (1991–2020) and end-of-century (2071–2100) conditions. When evaluating changes in nitrate concentration at the base of the mixed layer, we calculate total change (i.e., future nitrate concentration at the base of the future mixed layer minus historical nitrate concentration at the base of the historical mixed layer), and we also isolate the individual contributions of (a) MLD shoaling and (b) nitrate changes at constant depth. The former is estimated as the historical nitrate concentration at the future MLD minus the historical nitrate concentration at the historical MLD. The latter is estimated as the future nitrate concentration at the historical MLD minus the historical nitrate concentration at the historical MLD.

## 3. Results

### 3.1. Changes in Transport

Projected changes in upwelling magnitude (i.e., CUTI) are governed predominantly by two components — wind-driven Ekman transport and cross-shore geostrophic transport. In our ensemble of downscaled projections, we find a tendency toward increased upwelling-favorable Ekman transport in the northern half of the domain (Figure 2a), consistent with findings from global models (Rykaczewski et al., 2015). Changes in the southern half of the domain are more uncertain, with individual models showing increases or decreases, and the ensemble average showing little change in either direction, consistent with global models. Models are in closer agreement for projected changes in cross-shore geostrophic transport (Figure 2b), with modest changes in the northern part of the domain (>43°N) and larger changes off California that tend toward reduced onshore transport south of 37°N, also consistent with global models (Ding et al., 2021). The net effect of these changes is for model consensus on increased upwelling of ~10%–20% north of 41°N (owing primarily to Ekman transport) and south of 33°N (owing to both Ekman and geostrophic transports), with models disagreeing on the sign of change off central and northern California (34–41°N; Figure 2c; Figure S1 in Supporting Information S1).

### 3.2. Changes in Source Waters

While projections of change in EBUS often focus on the magnitude of upwelling, it is well established that changes in water column properties (e.g., stratification, MLD) and source water chemistry can alter nutrient availability and, consequently, the efficacy of upwelling. We find projected MLD decreases along the U.S. west coast that are robust across all three models, with the upwelling-season mean MLD shoaling throughout the



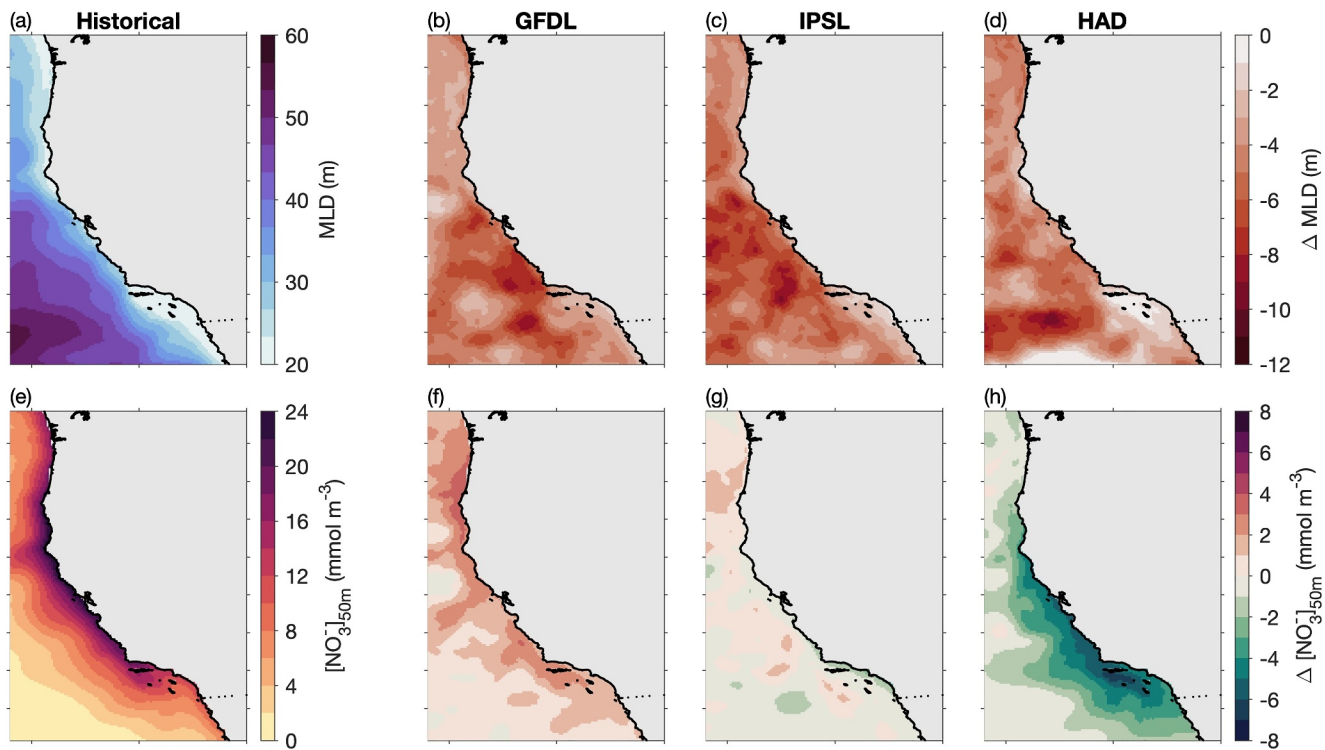


**Figure 3.** Historical (1991–2020) upwelling season (March–August) (a) mixed layer depth (MLD) and (e) nitrate concentration at 50 m depth from the ensemble average of downscaled simulations. Projected upwelling season changes between historical (1991–2020) and future (2071–2100) epochs in each of the three downscaled simulations for (b)–(d) MLD and (f)–(h) nitrate concentration. For MLD, negative changes indicate shoaling.

domain by up to 10 m over the 21st century under the high emissions RCP8.5 scenario (Figures 3b–3d). Both the historical mean MLD and the projected MLD change are several times greater in winter than in summer (mean MLD of ~40–60 m in winter, ~10–15 m in summer; MLD change of ~10–15 m in winter, ~0–5 m in summer). Projected shoaling of the mixed layer has been previously described in the literature, attributed to a sequence of events whereby increased radiative forcing drives surface-intensified heating, resulting in increased stratification, inhibition of mixing, and a shallower mixed layer (Alexander et al., 2018; Amaya et al., 2021; Capotondi et al., 2012; Cordero-Quiros et al., 2022).

Absent any changes in the vertical nitrate profile, this MLD shoaling would reduce nitrate concentration at the base of the mixed layer. However, global climate models also exhibit changes in nitrate concentration at depth (Figure S2 in Supporting Information S1), which are reflected in the downscaled simulations. Nitrate concentration at 50 m depth is projected to increase in the GFDL-forced simulation, decrease in the HAD-forced simulation, and change little in the IPSL-forced simulation (Figures 3f–3h), consistent with previous findings (Howard et al., 2020; Xiu et al., 2018). Thus, changes in MLD and nitrate concentration at depth can either reinforce (HAD) or counteract (GFDL) each other in terms of their contribution to nitrate at the base of the mixed layer. Isolating the relative contributions of each, we see that MLD shoaling is projected to reduce nitrate at the base of the mixed layer at all latitudes (Figure 4a), while the influence of nitrate changes at depth are highly model dependent (Figure 4b). In GFDL, where the two effects act in opposite directions, increased nitrate at depth dominates north of ~39°N while decreased nitrate due to MLD shoaling dominates farther south.

### 3.3. Changes in Nitrate Supply and Productivity

Projected changes in nitrate flux into the mixed layer (i.e., BEUTI) are latitude and model dependent (Figure 5c). In terms of absolute change, all models show small increases (decreases) at the most northern (southern) latitudes, while larger changes are projected along the California and Oregon coasts (~34–44°N), where IPSL and HAD exhibit reduced nitrate flux while GFDL projects an increase. In relative terms, the decreases at the southern end of the domain are dramatic (~30%–80%; considerably larger than relative changes in upwelling strength), as

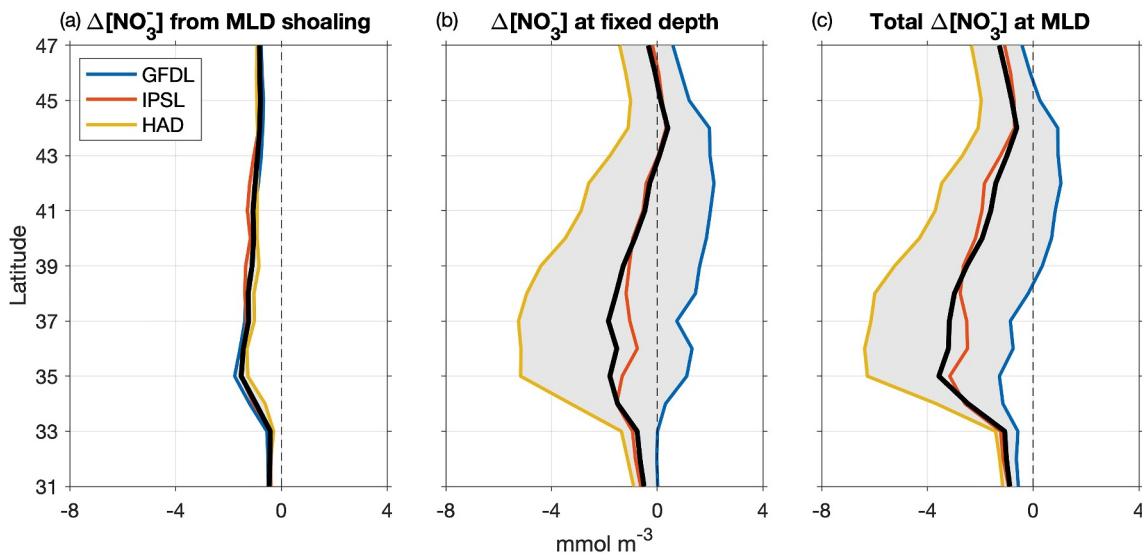


**Figure 4.** Contributions of (a) mixed layer depth (MLD) shoaling and (b) nitrate concentration changes at the historical MLD to (c) total change in nitrate concentration at the base of the mixed layer. Changes are calculated between historical (1991–2020) and future (2071–2100) epochs for the upwelling season (March–August). Each component is calculated as detailed in Section 2.3. Lines are as in Figure 2.

historical nitrate concentrations and fluxes are already very low in this region (Figures S1 and S3 in Supporting Information S1). Projected nitrate flux changes can result from changes in vertical transport or from alteration of the nitrate concentration in upwelled waters. In some cases, both factors act in the same direction (e.g., increasing for GFDL at most latitudes, decreasing for HAD off central and northern California). In other cases, the two effects oppose each other (e.g., increased upwelling but lower nitrate concentrations for IPSL throughout the domain). In most cases where upwelling strength and nitrate concentration trends are opposing, the latter has the dominant effect on trends in nitrate flux (i.e., the sign of change in BEUTI (Figure 5c) matches the sign of change in nitrate concentration (Figure 5b) more than it matches the sign of change in CUTI (Figure 5a)).

Projected changes in upwelling season phytoplankton biomass are similarly latitude and model dependent (Figure 5d), as has been shown in global models for the CCS and other EBUS (Bograd et al., 2023). Projected

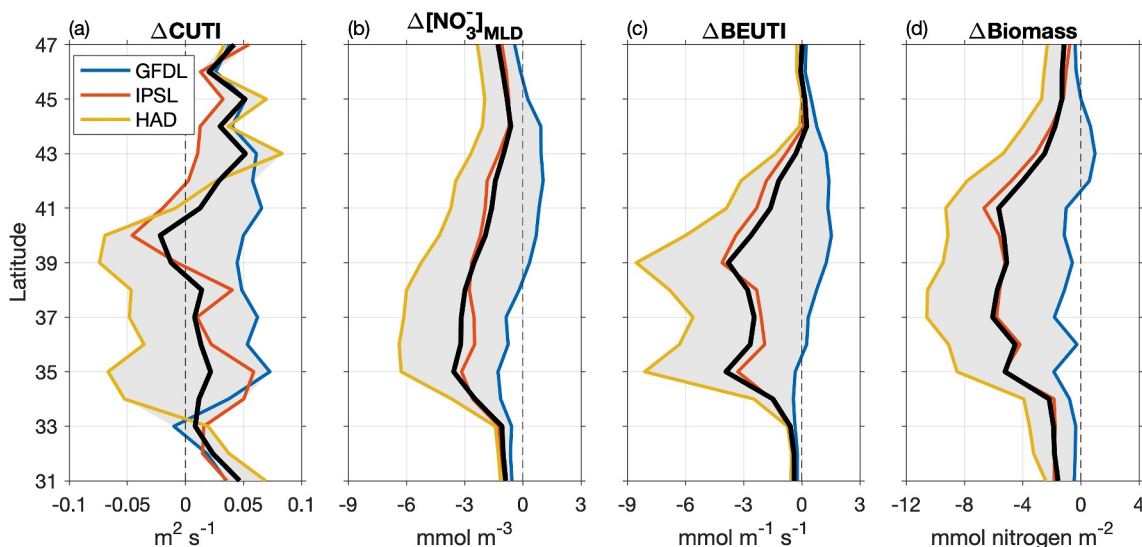


**Figure 5.** Projected upwelling season (March–August) changes in (a) total vertical transport (Coastal Upwelling Transport Index), (b) nitrate concentration at the base of the mixed layer, (c) nitrate flux into the mixed layer (Biologically Effective Upwelling Transport Index), and (d) phytoplankton biomass in the upper 50 m between historical (1991–2020) and future (2071–2100) epochs. Lines are as in Figure 2.

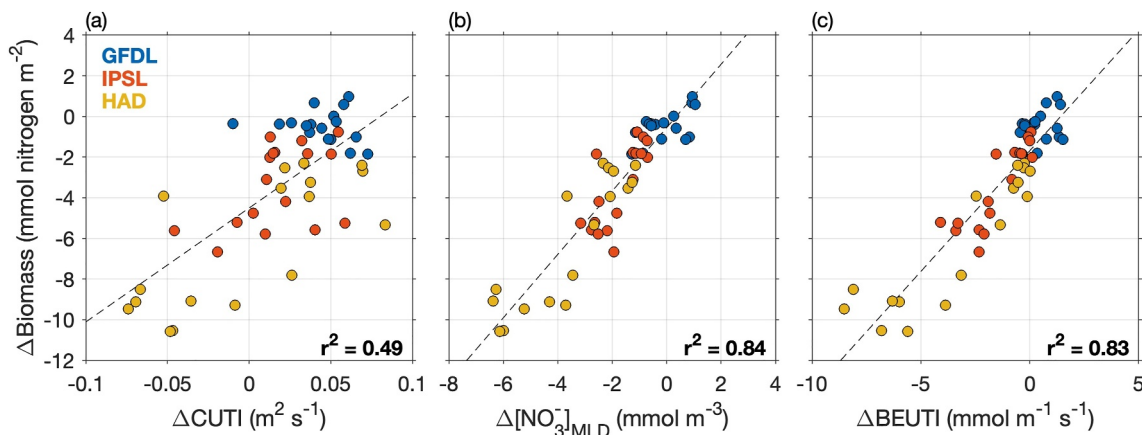


**Figure 6.** Projected upwelling season (March–August) changes in upper 50 m phytoplankton biomass as a function of changes in (a) vertical transport (Coastal Upwelling Transport Index), (b) nitrate concentration at the base of the mixed layer, and (c) nitrate flux into the mixed layer (Biologically Effective Upwelling Transport Index). Changes are calculated between historical (1991–2020) and future (2071–2100) epochs. Each circle represents a single 1° latitude region (Figure 1a) for a given model. Dashed lines are linear regressions, and r-squared values are shown in the lower right corner.

declines in biomass are evident in HAD and IPSL at all latitudes, with the greatest declines from 35 to 41°N. The only case of projected biomass increase is GFDL in the northern half of the domain. These overall biomass changes are dominated by large phytoplankton, which also dominate the mean biomass in the coastal upwelling region. Changes in small phytoplankton are of lower magnitude than those in large phytoplankton (Figure S4 in Supporting Information S1) and are generally of opposite sign, though the far northern (>45°N) and southern (<34°N) ends of the domain exhibit decreases in both size classes across all models (Figure S4 in Supporting Information S1).

Across models and latitudes, phytoplankton biomass changes are tightly coupled with changes in nitrate concentration and vertical nitrate flux at the base of the mixed layer ( $r^2 = 0.84$  and  $0.83$ , respectively) and much less so with changes in upwelling strength ( $r^2 = 0.49$ ) (Figure 6). This finding is robust when looking at the full seasonal evolution of projected changes as well (Figure S3 in Supporting Information S1); phytoplankton biomass changes directly reflect changes in the upwelled nutrient supply but not necessarily in the strength of upwelling. Indeed, all three models exhibit regions and times of year where phytoplankton biomass declines despite stronger upwelling. However, changes in biomass are not necessarily proportional to changes in nitrate supply. In the northern half of the domain, nitrate flux and phytoplankton biomass have comparable relative changes of ~0%–30%. In contrast, in the southern portion of the domain, nitrate flux reductions that are relatively small in magnitude can be large in a relative sense (~30%–80%), far exceeding the relative biomass changes (~0%–30%).

#### 4. Discussion

Despite considerable interest in quantifying future physical and biogeochemical changes in EBUS, few (if any) studies have thoroughly explored projected changes in the full suite of atmospheric and oceanic conditions relevant to the fate of upwelling-driven productivity in these regions. Here, we used an ensemble of regionally downscaled ocean projections for the CCS to explore the model-, latitude-, and season-dependent influences of climate change on Ekman transport, geostrophic transport, MLD, and subsurface nitrate concentrations. We find locations, times, and variables for which the models agree, and others for which there is considerable model uncertainty with no consensus on even the sign of future change. However, despite the lack of consensus on future changes, there is agreement across models, seasons, and latitudes that projected changes in phytoplankton biomass are driven by nutrient supply. Furthermore, in all models the dominant driver of changes in nitrate supply is not upwelling strength, but rather the nitrate concentration of upwelled water.

There are obvious potential extensions to this work, including the use of additional future climate scenarios, ESMs, and regional ocean-biogeochemical models. Each would allow for greater exploration of the uncertainty in projected primary production and its drivers. However, the suite of models chosen here under the high-emissions scenario bounds the uncertainty in primary production under lower emissions scenarios (Poza Buil et al., 2021), and physical and biogeochemical responses under lower emissions scenarios are likely to be qualitatively similar

but with lower magnitude (Bograd et al., 2023). Furthermore, the fact that the downscaled biogeochemical changes mirror those in the parent ESMs indicates that the use of a single regional model is allowing for better resolution but is not fundamentally affecting our results (note Echevin et al. (2020) found that biogeochemical trends were different between global and downscaled models in the Peru upwelling system). Additional impacts to explore include the role of changing freshwater forcing, other macro- and micro-nutrients (e.g., iron), and potential transport-related impacts (e.g., more rapid offshore advection associated with a shoaling mixed layer; Jung & Cho, 2023).

Starting with the Bakun (1990) hypothesis about anthropogenic increases in coastal upwelling, much of the focus on future change in EBUS has been on upwelling itself. However, we find that the strength of upwelling, while important, is not the dominant driver of projected changes in nitrate flux, nor the resultant changes in phytoplankton biomass. Our results suggest that increased attention to subsurface nutrient changes is warranted, particularly for the dynamics driving diverging model projections. Better constraining ESM changes in source water chemistry is key to lowering the uncertainty in projections of primary production and associated higher trophic level impacts.

### Data Availability Statement

Output from the downscaled projections of the CCS is available at the NOAA Climate Change Portal (<https://psl.noaa.gov/ipcc/ccs/>) and at NOAA ERDDAP (<https://oceanview.pfeg.noaa.gov/erddap/search/index.html?searchFor=CCS%20ROMS>). Projected upwelling indices (CUTI and BEUTI) from each of the downscaled ocean projections are available at Jacox (2024).

### Acknowledgments

We thank the NOAA Modeling, Analysis, Predictions, and Projections program (NA200AR4310447) for funding support. We appreciate comments from anonymous peer review for guiding improvements to the manuscript.

### References

- Alexander, M. A., Scott, J. D., Friedland, K. D., Mills, K. E., Nye, J. A., Pershing, A. J., & Thomas, A. C. (2018). Projected sea surface temperatures over the 21st century: Changes in the mean, variability and extremes for large marine ecosystem regions of Northern Oceans. *Elementa: Science of the Anthropocene*, 6, 9. <https://doi.org/10.1525/elementa.191>
- Amaya, D. J., Alexander, M. A., Capotondi, A., Deser, C., Karnauskas, K. B., Miller, A. J., & Mantua, N. J. (2021). Are long-term changes in mixed layer depth influencing North Pacific marine heatwaves? *Bulletin of the American Meteorological Society*, 102(1), S59–S66. <https://doi.org/10.1175/bams-d-20-0144.1>
- Atlas, R., Hoffman, R. N., Ardizzone, J., Leidner, S. M., Jusem, J. C., Smith, D. K., & Gombos, D. (2011). A cross-calibrated, multiplatform ocean surface wind velocity product for meteorological and oceanographic applications. *Bulletin of the American Meteorological Society*, 92(2), 157–174. <https://doi.org/10.1175/2010bams2946.1>
- Bakun, A. (1990). Global climate change and intensification of coastal ocean upwelling. *Science*, 247(4939), 198–201. <https://doi.org/10.1126/science.247.4939.198>
- Bograd, S. J., Jacox, M. G., Hazen, E. L., Lovecchio, E., Montes, I., Pozo Buil, M., et al. (2023). Climate change impacts on eastern boundary upwelling systems. *Annual Review of Marine Science*, 15(1), 303–328. <https://doi.org/10.1146/annurev-marine-032122-021945>
- Capotondi, A., Alexander, M. A., Bond, N. A., Curchitser, E. N., & Scott, J. D. (2012). Enhanced upper ocean stratification with climate change in the CMIP3 models. *Journal of Geophysical Research*, 117(C4), C04031. <https://doi.org/10.1029/2011jc007409>
- Carton, J. A., & Giese, B. S. (2008). A reanalysis of ocean climate using Simple Ocean Data Assimilation (SODA). *Monthly Weather Review*, 136(8), 2999–3017. <https://doi.org/10.1175/2007mwr1978.1>
- Chang, P., Xu, G., Kurian, J., Small, R. J., Danabasoglu, G., Yeager, S., et al. (2023). Uncertain future of sustainable fisheries environment in eastern boundary upwelling zones under climate change. *Communications Earth & Environment*, 4(1), 19. <https://doi.org/10.1038/s43247-023-00681-0>
- Cheresh, J., & Fiechter, J. (2020). Physical and biogeochemical drivers of alongshore pH and oxygen variability in the California Current System. *Geophysical Research Letters*, 47(19), e2020GL089553. <https://doi.org/10.1029/2020gl089553>
- Cheresh, J., Kroeker, K. J., & Fiechter, J. (2023). Upwelling intensity and source water properties drive high interannual variability of corrosive events in the California Current. *Scientific Reports*, 13(1), 13013. <https://doi.org/10.1038/s41598-023-39691-5>
- Colas, F., Capet, X., McWilliams, J. C., & Shepetchkin, A. (2008). 1997–1998 El Niño off Peru: A numerical study. *Progress in Oceanography*, 79(2–4), 138–155. <https://doi.org/10.1016/j.pocean.2008.10.015>
- Cordero Quirós, N., Jacox, M. G., Pozo Buil, M., & Bograd, S. J. (2022). Future changes in eddy kinetic energy in the California Current System from dynamically downscaled climate projections. *Geophysical Research Letters*, 49(21), e2022GL099042. <https://doi.org/10.1029/2022gl099042>
- Deutsch, C., Frenzel, H., McWilliams, J. C., Renault, L., Kessouri, F., Howard, E., et al. (2021). Biogeochemical variability in the California Current system. *Progress in Oceanography*, 196, 102565. <https://doi.org/10.1016/j.pocean.2021.102565>
- Ding, H., Alexander, M. A., & Jacox, M. G. (2021). Role of geostrophic currents in future changes of coastal upwelling in the California Current System. *Geophysical Research Letters*, 48(3), e2020GL090768. <https://doi.org/10.1029/2020gl090768>
- Doney, S. C., Ruckelshaus, M., Emmett Duffy, J., Barry, J. P., Chan, F., English, C. A., et al. (2012). Climate change impacts on marine ecosystems. *Annual Review of Marine Science*, 4(1), 11–37. <https://doi.org/10.1146/annurev-marine-041911-111611>
- Drenkard, E. J., Stock, C., Ross, A. C., Dixon, K. W., Adcroft, A., Alexander, M., et al. (2021). Next-generation regional ocean projections for living marine resource management in a changing climate. *ICES Journal of Marine Science*, 78(6), 1969–1987. <https://doi.org/10.1093/icesjms/fsab100>
- Echevin, V., Gévaudan, M., Espinoza-Morriberón, D., Tam, J., Aumont, O., Gutierrez, D., & Colas, F. (2020). Physical and biogeochemical impacts of RCP8.5 scenario in the Peru upwelling system. *Biogeosciences*, 17(12), 3317–3341. <https://doi.org/10.5194/bg-17-3317-2020>



- Fiechter, J., Edwards, C. A., & Moore, A. M. (2018). Wind, circulation, and topographic effects on alongshore phytoplankton variability in the California Current. *Geophysical Research Letters*, *45*(7), 3238–3245. <https://doi.org/10.1002/2017gl076839>
- Garcia, H., Locarnini, R., Boyer, T., Antonov, J., Baranova, O., Zweng, M., et al. (2010). Dissolved oxygen, apparent oxygen utilization, and oxygen saturation. Vol. 3, World Ocean Atlas 2009. *NOAA Atlas Nesdis* (Vol. 70, p. 28).
- Garcia, H., Locarnini, R., Boyer, T., Antonov, J., Zweng, M., Baranova, O., et al. (2010). In S. Levitus (Ed.), *World Ocean Atlas 2009, volume 4: Nutrients (phosphate, nitrate, silicate)*, NOAA Atlas NESDIS 71. U.S. Government Printing Office.
- García-Reyes, M., Sydeman, W. J., Schoeman, D. S., Rykaczewski, R. R., Black, B. A., Smit, A. J., & Bograd, S. J. (2015). Under pressure: Climate change, upwelling, and eastern boundary upwelling ecosystems. *Frontiers in Marine Science*, *2*, 109. <https://doi.org/10.3389/fmars.2015.00109>
- Hersbach, H., Bell, B., Berrisford, P., Hirahara, S., Horányi, A., Muñoz-Sabater, J., et al. (2020). The ERA5 global reanalysis. *Quarterly Journal of the Royal Meteorological Society*, *146*(730), 1999–2049. <https://doi.org/10.1002/qj.3803>
- Howard, E. M., Frenzel, H., Kessouri, F., Renault, L., Bianchi, D., McWilliams, J. C., & Deutsch, C. (2020). Attributing causes of future climate change in the California Current System with multimodel downscaling. *Global Biogeochemical Cycles*, *34*(11), e2020GB006646. <https://doi.org/10.1029/2020gb006646>
- Jacox, M. G. (2024). Upwelling index projections - CMIP5 RCP8 (Vol. 5) [Dataset]. *Zenodo*. <https://doi.org/10.5281/zenodo.10887772>
- Jacox, M. G., Edwards, C. A., Hazen, E. L., & Bograd, S. J. (2018). Coastal upwelling revisited: Ekman, Bakun, and improved upwelling indices for the US West Coast. *Journal of Geophysical Research: Oceans*, *123*(10), 7332–7350. <https://doi.org/10.1029/2018jc014187>
- Jacox, M. G., Hazen, E. L., & Bograd, S. J. (2016). Optimal environmental conditions and anomalous ecosystem responses: Constraining bottom-up controls of phytoplankton biomass in the California Current System. *Scientific Reports*, *6*(1), 27612. <https://doi.org/10.1038/srep27612>
- Jing, Z., Wang, S., Wu, L., Wang, H., Zhou, S., Sun, B., et al. (2023). Geostrophic flows control future changes of oceanic eastern boundary upwelling. *Nature Climate Change*. <https://doi.org/10.1038/s41558-022-01588-y>
- Jung, J., & Cho, Y. K. (2023). Effects of surface heating on coastal upwelling intensity. *Journal of Geophysical Research: Oceans*, *128*(2), e2022JC018795. <https://doi.org/10.1029/2022jc018795>
- Kara, A. B., Rochford, P. A., & Hurlburt, H. E. (2000). An optimal definition for ocean mixed layer depth. *Journal of Geophysical Research*, *105*(C7), 16803–16821. <https://doi.org/10.1029/2000jc900072>
- Kishi, M. J., Kashiwai, M., Ware, D. M., Megrey, B. A., Werner, F. E., Eslinger, D. L., et al. (2007). NEMURO—A lower trophic level model for the North Pacific marine ecosystem. *Ecological Modelling*, *202*(1–2), 12–25. <https://doi.org/10.1016/j.ecolmodel.2006.08.021>
- Marchesiello, P., & Estrade, P. (2010). Upwelling limitation by onshore geostrophic flow. *Journal of Marine Research*, *68*(1), 37–62. <https://doi.org/10.1357/002224010793079004>
- Messié, M., & Chavez, F. P. (2015). Seasonal regulation of primary production in eastern boundary upwelling systems. *Progress in Oceanography*, *134*, 1–18. <https://doi.org/10.1016/j.pocean.2014.10.011>
- Oerder, V., Colas, F., Echevin, V., Codron, F., Tam, J., & Belmadani, A. (2015). Peru-Chile upwelling dynamics under climate change. *Journal of Geophysical Research: Oceans*, *120*(2), 1152–1172. <https://doi.org/10.1002/2014jc010299>
- Pozo Buil, M., Jacox, M. G., Fiechter, J., Alexander, M. A., Bograd, S. J., Curchitser, E. N., et al. (2021). A dynamically downscaled ensemble of future projections for the California current system. *Frontiers in Marine Science*, *8*, 612874. <https://doi.org/10.3389/fmars.2021.612874>
- Rykaczewski, R. R., & Dunne, J. P. (2010). Enhanced nutrient supply to the California Current Ecosystem with global warming and increased stratification in an earth system model. *Geophysical Research Letters*, *37*(21), L21606. <https://doi.org/10.1029/2010gl045019>
- Rykaczewski, R. R., Dunne, J. P., Sydeman, W. J., García-Reyes, M., Black, B. A., & Bograd, S. J. (2015). Poleward displacement of coastal upwelling-favorable winds in the ocean's eastern boundary currents through the 21st century. *Geophysical Research Letters*, *42*(15), 6424–6431. <https://doi.org/10.1002/2015gl064694>
- Schmidt, D. F., Amaya, D. J., Grise, K. M., & Miller, A. J. (2020). Impacts of shifting subtropical highs on the California Current and Canary Current systems. *Geophysical Research Letters*, *47*(15), e2020GL088996. <https://doi.org/10.1029/2020gl088996>
- Shi, H., Jin, F. F., Wills, R. C., Jacox, M. G., Amaya, D. J., Black, B. A., et al. (2022). Global decline in ocean memory over the 21st century. *Science Advances*, *8*(18), eabm3468. <https://doi.org/10.1126/sciadv.abm3468>
- Veneziani, M., Edwards, C. A., Doyle, J. D., & Foley, D. (2009). A central California coastal ocean modeling study: 1. Forward model and the influence of realistic versus climatological forcing. *Journal of Geophysical Research*, *114*(C4), C04015. <https://doi.org/10.1029/2008jc004774>
- Wang, D., Gouhier, T. C., Menge, B. A., & Ganguly, A. R. (2015). Intensification and spatial homogenization of coastal upwelling under climate change. *Nature*, *518*(7539), 390–394. <https://doi.org/10.1038/nature14235>
- Xiu, P., Chai, F., Curchitser, E. N., & Castruccio, F. S. (2018). Future changes in coastal upwelling ecosystems with global warming: The case of the California Current System. *Scientific Reports*, *8*(1), 2866. <https://doi.org/10.1038/s41598-018-21247-7>